Electronic Supplementary Material (ESI) for Chemical Communications

Supporting Information

for

A doubly 2,6-pyridylene-bridged porphyrin-perylene-porphyrin triad

Shin Ikeda,[a] Naoki Aratani[a,b]* and Atsuhiro Osuka[a]*

[a]*Department of Chemistry, Graduate School of Science, Kyoto University, Sakyo-ku, Kyoto 606-8502 (Japan)*

[b]*PRESTO, Japan Science and Technology Agency (Japan)*

E-mail: aratani@kuchem.kyoto-u.ac.jp; osuka@kuchem.kyoto-u.ac.jp

Contents

1. Instrumentation and Materials

All solvents for reaction were distilled over CaH_2. All reagents were of the commercial reagent grade and were used without further purification except where noted. The spectroscopic grade dichloromethane was used as solvent for all spectroscopic studies. Preparative separations were performed by silica gel gravity column chromatography (Wakogel C-300) or size exclusion gel permeation chromatography (GPC) (Bio-Rad Bio-Beads S-X1, packed with $CHCl_3$). Thin-layer chromatography (TLC) was carried out on aluminum sheets coated with silica gel 60 F_{254} (Merck 5554). UV-visible spectra were recorded on a Shimadzu UV-3100PC spectrometer. Steady–state fluorescence emission spectra were recorded on a Shimadzu RF-5300PC spectrometer. Absolute quantum yields were determined with a Hamamatsu C9920-01 calibrated integrating sphere system. ^1H spectra were recorded on a JEOL ECA-600 spectrometer (operating as 600.17 MHz for ^1H) using the residual solvent as the internal reference for ^1H (δ = 7.26 ppm in $CDCl_3$). High-resolution electrospray-ionization time-of-flight mass spectroscopy (HR-ESI-TOF-MS) for **5Ni** and **5Zn** was recorded on a BRUKER micrOTOF model using positive mode for acetonitrile solutions of samples. Mass spectrum for **5H** was recorded on a Shimadzu AXIMA-CFRplus using positive-MALDI-TOF method with matrix. Redox potentials were measured by cyclic and differential pulse voltammetry on an ALS electrochemical analyzer model 660 (Bu_4NPF_6 electrolyte 0.1 M in CH_2Cl_2, Ag/$AgClO_4$ reference electrode, Pt wire counter electrode, glassy carbon working electrode, scan rate 0.05 V/s). Crystallographic data were collected on a Rigaku RAXIS–RAPID apparatus at –180 °C using graphite-monochromated CuKα radiation (λ = 1.54187 Å). The structures were solved by direct methods (SHELXS-97) and refined with full-matrix least square technique (SHELXL-97).[S1]

Synthesis

2,5,8,11-Tetrakis(6-bromopyrid-2-yl)perylene 3: A toluene–DMF solution (10 mL/10 mL) of 2,5,8,11-Tetraborylperylene **2**[S2] (151 mg, 0.20 mmol), 2,6-dibromopyridine (1.41 g, 6.0 mmol), $Pd_2(dba)_3$ (18 mg, 0.020 mmol), PPh_3 (21 mg, 0.080 mmol), Cs_2CO_3 (260 mg, 0.80 mmol) and CsF (120 mg, 0.80 mmol) was degassed through three freeze-pump-thaw cycles, and the reaction flask was purged with argon. The resulting mixture was stirred at refluxed temperature for 48 h. The reaction mixture was diluted with $CHCl_3$, washed with water, and **3** was obtained as a green solid (129 mg, 0. 14 mmol, 73% yield). ^1H NMR ($CDCl_3$) δ 8.91 (s, 4H, perylene), 8.52 (t, J = 8.3 Hz, 4H, py), 8.49 (s, 4H, perylene), 8.42 (d, J = 7.3 Hz, 4H, py), 8.16 (d, J = 8.3 Hz, 4H, py).

2,6-Pyridylene-bridged porphyrin-perylene triad 5Ni: A toluene–DMF solution (14 mL/7 mL) of **4**[S3] (59 mg, 0.050 mmol), **3** (22 mg, 0.025 mmol), $Pd_2(dba)_3$ (4.6 mg, 0.0050 mmol), PPh_3 (5.2 mg, 0.020 mmol), Cs_2CO_3 (33 mg, 0.10 mmol), and CsF (13 mg, 0.10 mmol) was degassed through three freeze-pump-thaw cycles, and the reaction flask was purged with argon. The resulting mixture was stirred at reflux for 17.5 h. The reaction mixture was diluted with CH_2Cl_2, washed with water, and the organic layer was dried over anhydrous sodium sulfate. After evaporation of the solvent followed by GPC and silica-gel column chromatography ($CHCl_3$ as an eluent) and recrystallization with CH_2Cl_2/MeOH, **5Ni** was obtained as a red solid (8.6 mg, 3.5 μmol, 14% yield). ^{1}H NMR ($CDCl_3$, 60 °C) δ 10.71 (s, 2H, *meso*), 9.78 (s, 4H, perylene), 8.92 (s, 4H, β), 8.69 (s, 8H, β), 8.09 (d, J = 7.2 Hz, 8H, py + perylene), 7.98 (t, J = 8.1 Hz, 4H, py), 7.81 (s, 12H, Ar-*o*), 7.78 (d, J = 7.8 Hz, 4H, py), 7.71 (s, 4H, Ar-*p*), 7.68 (s, 2H, Ar-*p*), 1.47 (s, 72H, ^{t}Bu), 1.44 (s, 36H, ^{t}Bu). HR-ESI-TOF-MS m/z = 1209.0845, calcd for $C_{164}H_{160}N_{12}Ni_2$ = 1209.0868 $[M]^{2+}$; UV-Vis (CH_2Cl_2) λ_{max} (ε [$M^{-1}cm^{-1}$]) = 430 (400000) and 546 (31000) nm.

2,6-Pyridylene-bridged porphyrin-perylene-porphyrin triad free base 5H: **5Ni** (2.3 mg, 0.95 μmol) was dissolved in TFA and several drops of H_2SO_4 were added. After being refluxed for 6 h, the mixture was diluted with CH_2Cl_2 and neutralized with $NaHCO_3$ aq., and the organic layer was dried over anhydrous sodium sulfate. After evaporation, **5H** was obtained as a red solid. ^{1}H NMR ($CDCl_3$) δ 11.25 (s, 2H, *meso*), 10.03 (s, 4H, perylene), 9.05 (s, 4H, β), 8.91 (d, J = 5.4 Hz, 4H, β), 8.84 (d, J = 5.4 Hz, 4H, β), 8.25 (br, 4H, py), 8.07-8.10 (m, 12H), 7.93 (br, 4H, py), 7.81 (s, 4H, Ar-*p*), 7.77 (s, 4H, Ar-*p*), –2.15 (s, 2H, NH) and –2.39 (s, 2H, NH). MALDI-TOF-MS m/z = 2302.3205, calcd for $C_{164}H_{164}N_{12}$ = 2302.3226 $[M]^+$; UV-Vis (CH_2Cl_2) λ_{max} (ε [$M^{-1}cm^{-1}$]) = 427 (610000) and 522 (33000) nm.

2,6-Pyridylene-bridged porphyrin-perylene-porphyrin triad zinc(II) complex 5Zn: A $CHCl_3$-MeOH solution (20 ml/1 ml) of **5H** (3.6 mg, 1.5 μmol) and $Zn(OAc)_2{\cdot}(H_2O)_2$ (6.1 mg) was stirred at refluxed temperature for 2 h. The mixture was diluted with CH_2Cl_2 and neutralized with $NaHCO_3$ aq., and the organic layer was dried over anhydrous sodium sulfate. After evaporation, **5Zn** was obtained as a red solid. ^{1}H NMR ($CDCl_3$) δ 11.34 (s, 2H, *meso*), 10.03 (s, 4H, perylene), 9.16 (s, 4H, β), 9.01 (d, J = 5.4 Hz, 4H, py), 8.97 (d, J = 5.4 Hz, 4H, β), 8.27 (s, 4H, perylene), 8.14-8.07 (m, 20H), 7.92 (d, J = 8.4 Hz, 4H, py), 7.80 (s, 4H, Ar-*p*), and 7.77 (s, 4H, Ar-*p*). HR-ESI-TOF-MS m/z = 2430.1502, calcd for $C_{164}H_{160}N_{12}Zn_2$ = 2430.1579 $[M]^+$; UV-Vis (CH_2Cl_2) λ_{max} (ε [$M^{-1}cm^{-1}$]) = 429 (731000) and 553 (11000) nm.

2. ^{1}H NMR Spectra

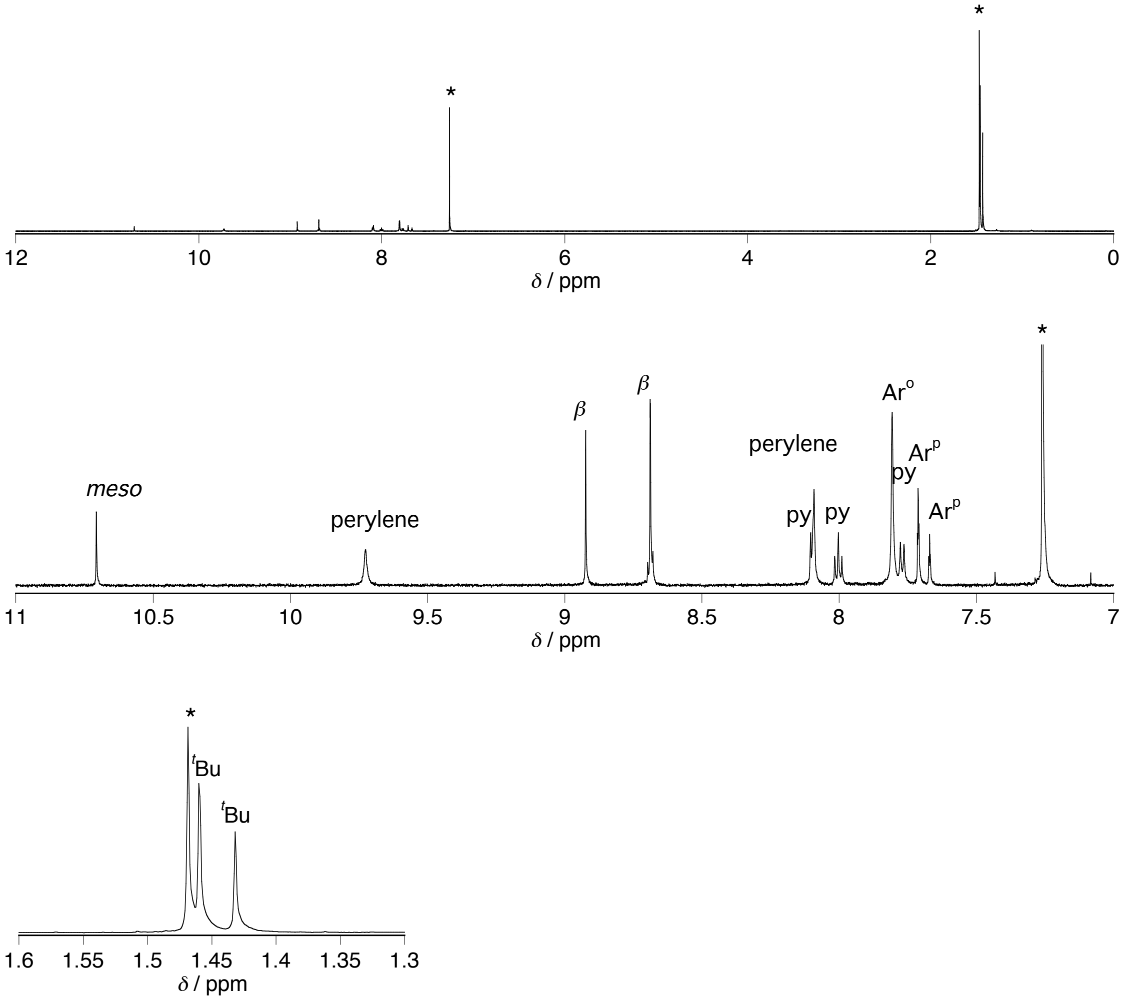

Figure S1. ^{1}H NMR spectrum of (a) **5Ni** in $CDCl_3$ at 60°C.
(* means solvent residual peaks or impurities.)

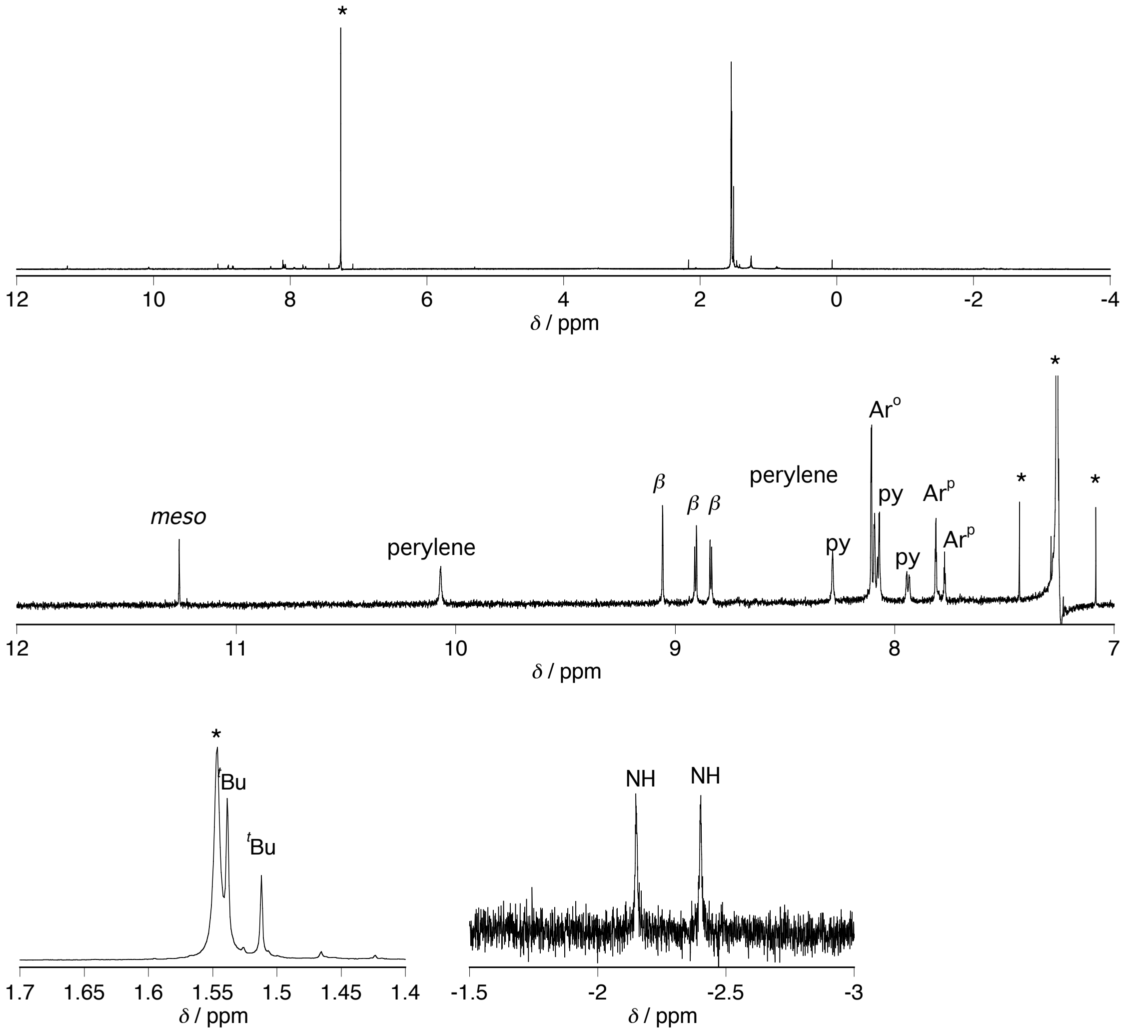

Figure S2. ^{1}H NMR spectrum of **5H** in $CDCl_3$ at room temperature.
(* means solvent residual peaks or impurities.)

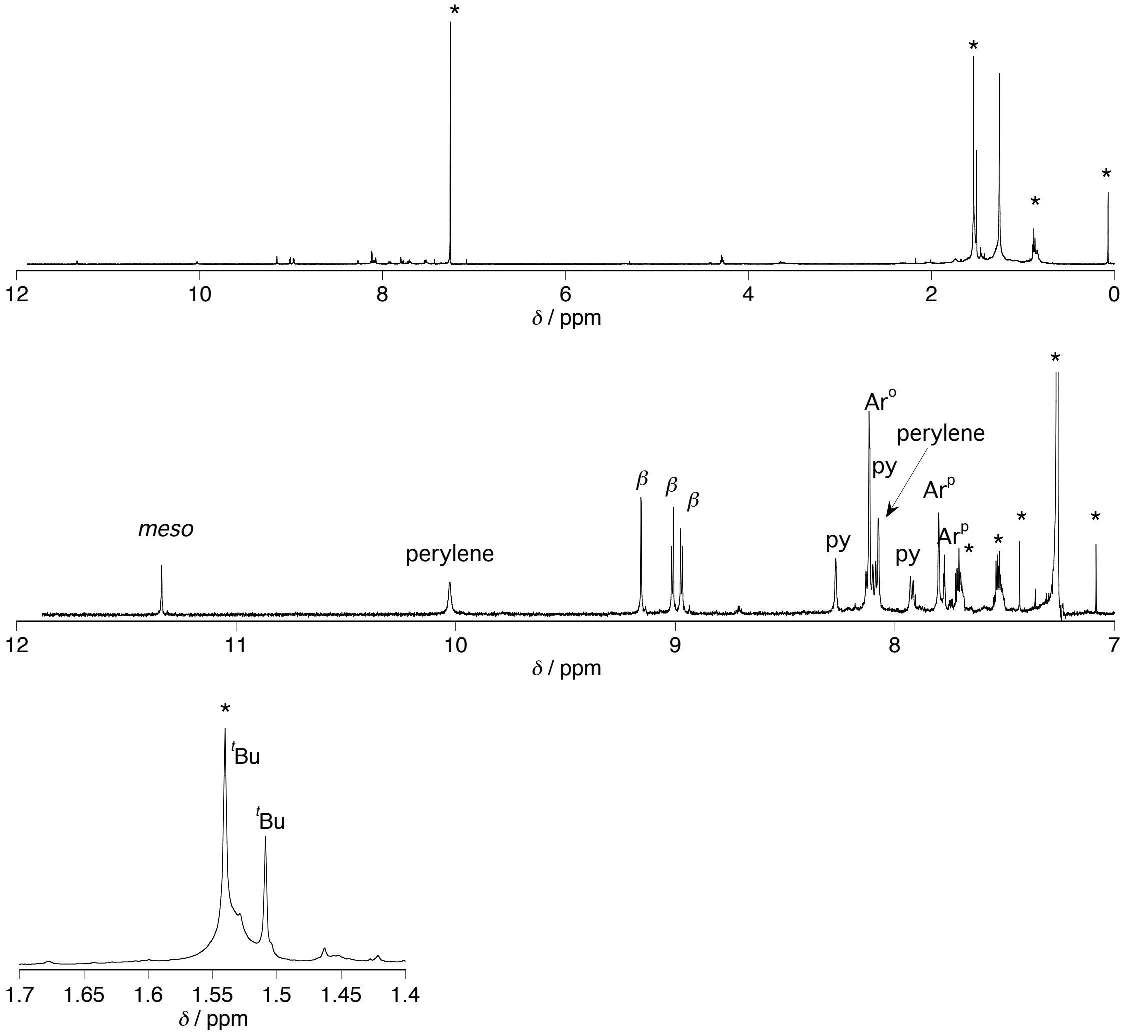

Figure S3. ^{1}H NMR spectrum of **5Zn** in $CDCl_3$ at room temperature.
(* means solvent residual peaks or impurities.)

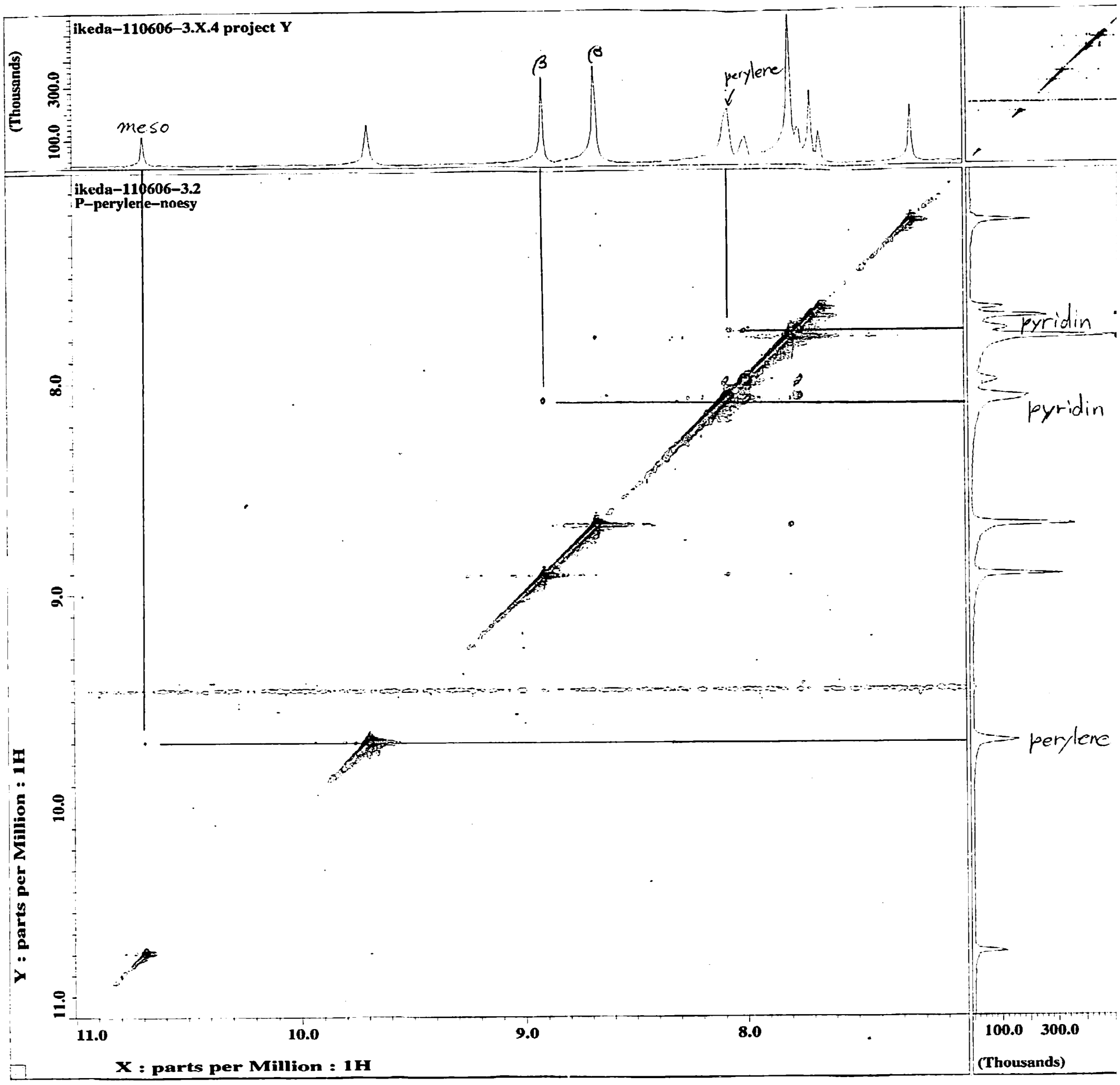

Figure S4. ^{1}H-^{1}H NOESY chart of **5Ni** in $CDCl_3$ at 60 °C.

3. Mass Spectra

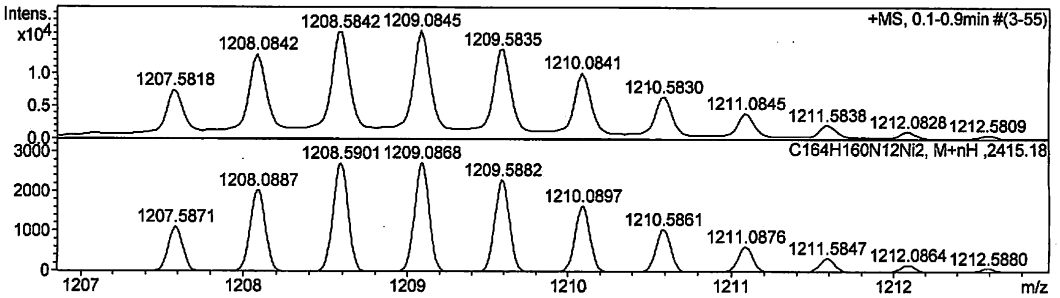

Figure S5. HR-ESI-TOF-MS of **5Ni** (positive ion mode).

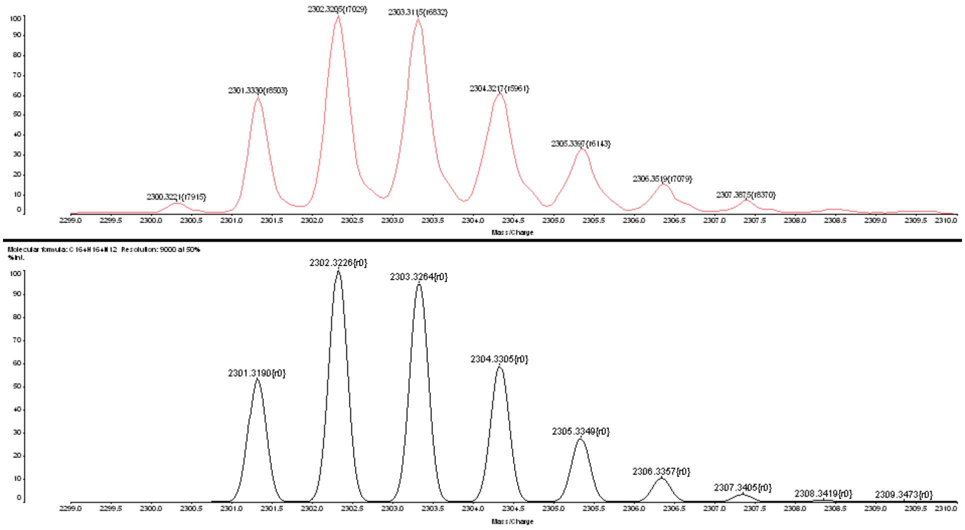

Figure S6. HR-MALDI-TOF-MS of **5H** (positive ion mode).

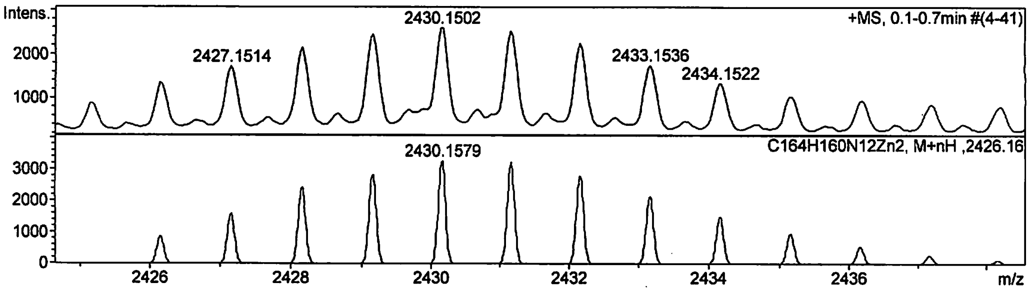

Figure S7. HR-ESI-TOF-MS of **5Zn** (positive ion mode).

4. Complexation Experiments

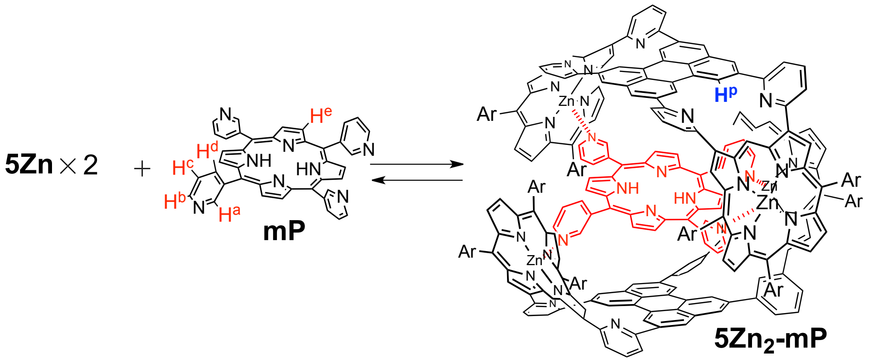

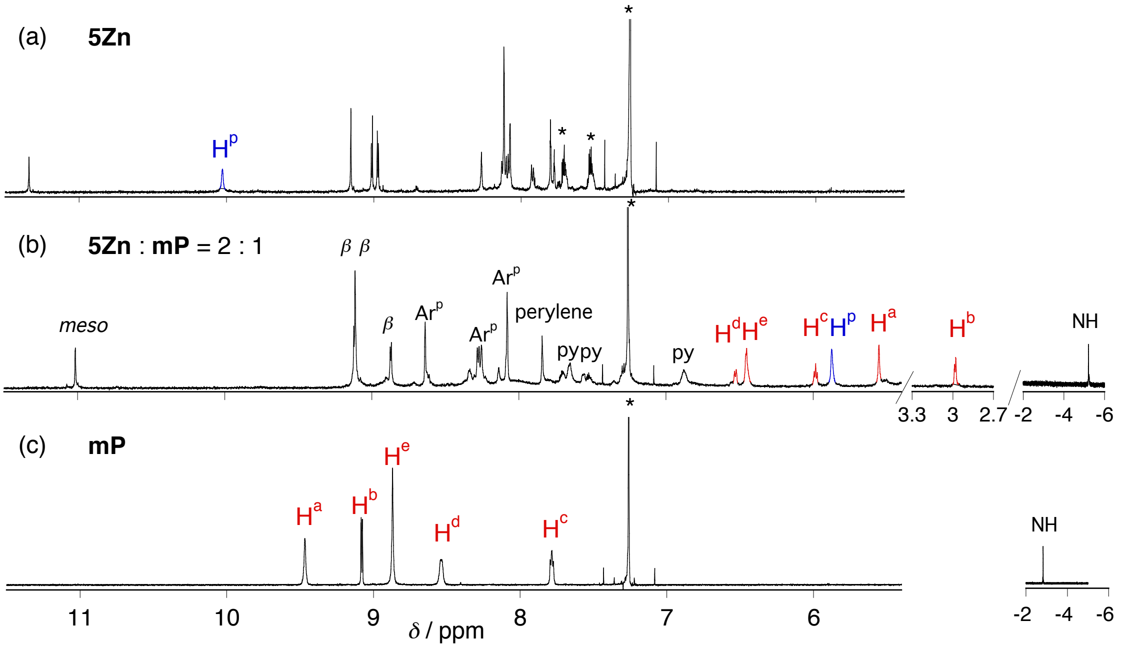

Figure S8. ^{1}H NMR spectra of (a) **5Zn**, (b) **$5Zn_2$–mP** and (c) **mP** in $CDCl_3$ at room temperature. (* means solvent residual peaks or impurities.)

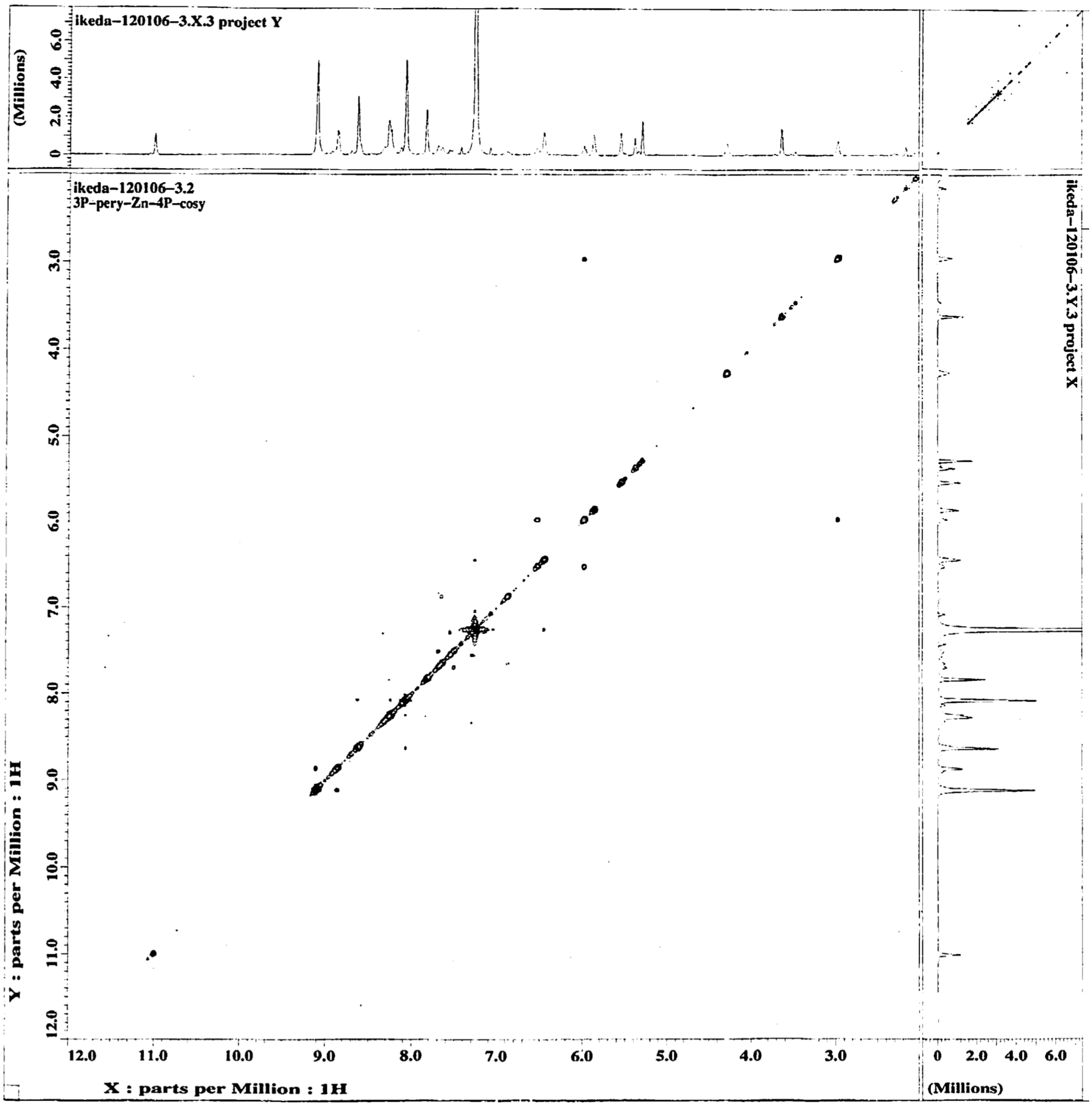

Figure S9. ^{1}H-^{1}H COSY chart of **5Zn$_2$–mP** in CDCl$_3$ at room temperature.

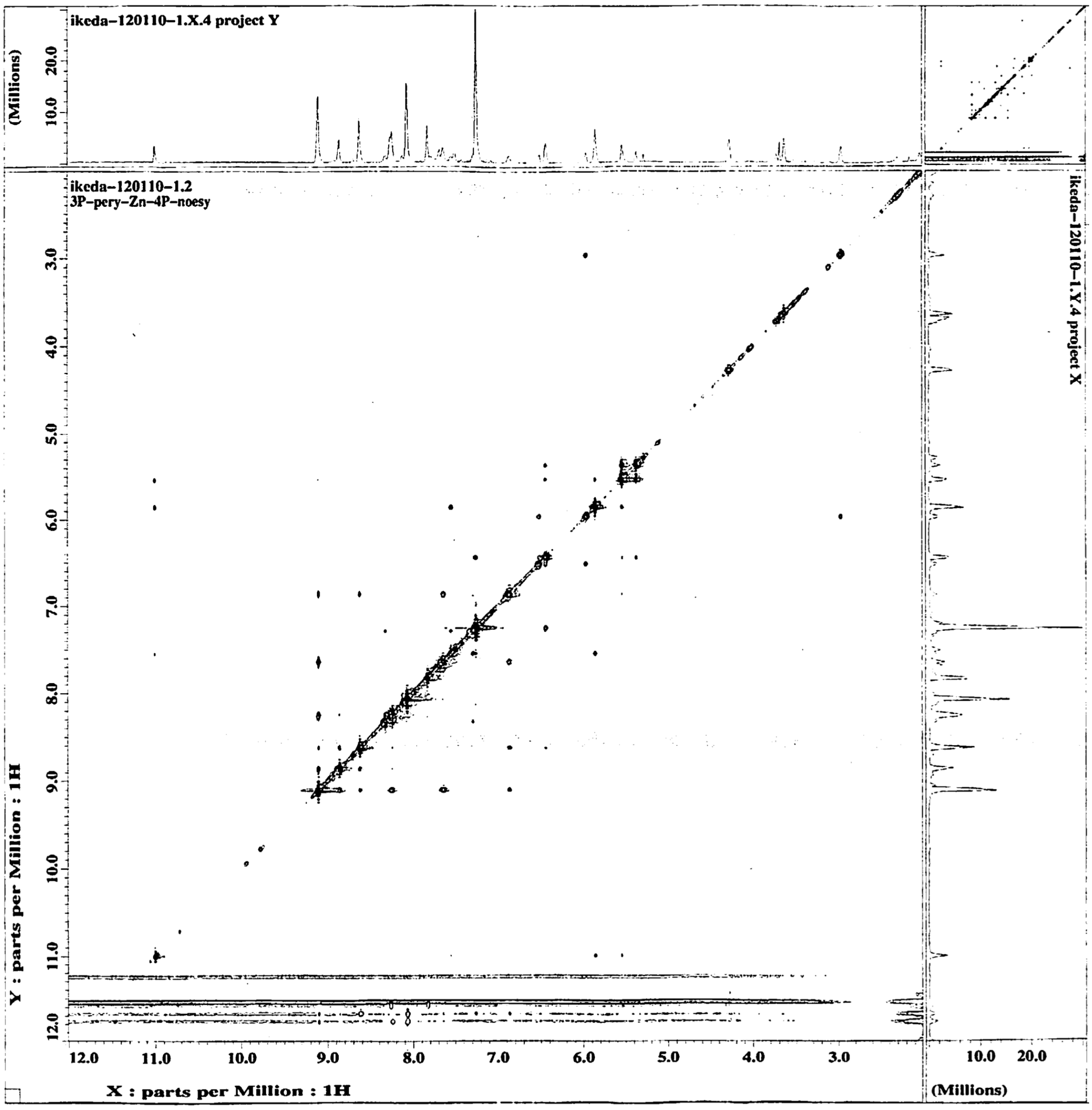

Figure S10. ^1H-^1H NOESY chart of **$5Zn_2$–mP** in $CDCl_3$ at room temperature.

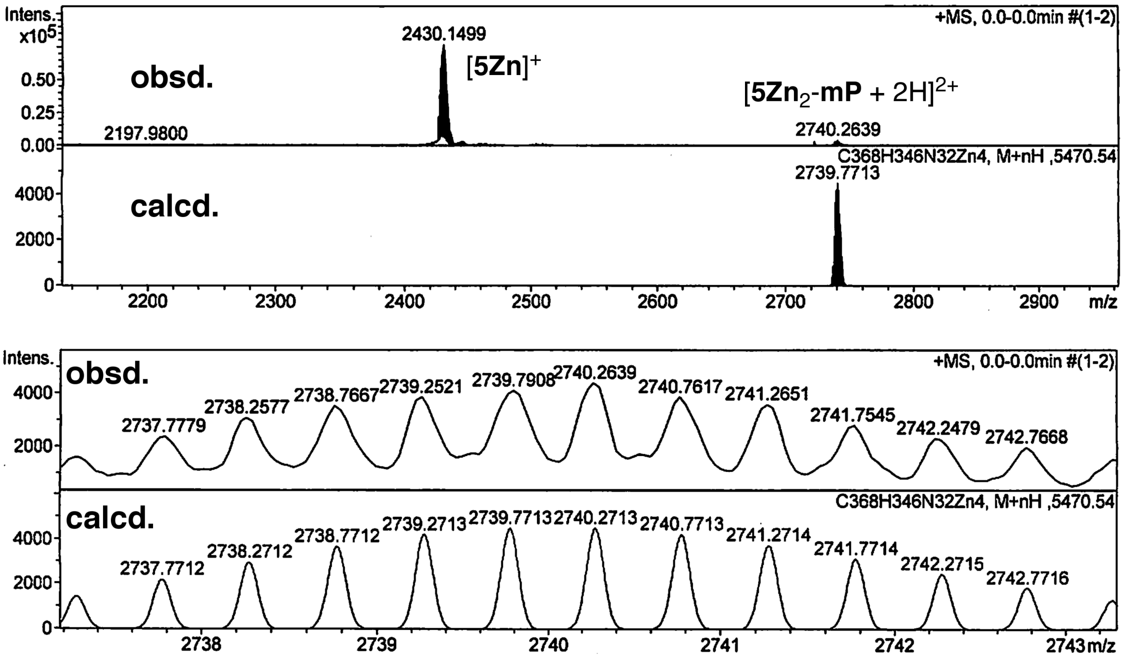

Figure S11. HR-ESI-TOF-MS of **5Zn$_2$–mP** (positive ion mode).

UV-vis. studies of 5Zn with mP and Job's plot

Solutions of **5Zn** and **mP** were mixed to prepare 15 samples with varying mole fractions of **5Zn** from 0 to 1, which were subjected to UV-vis spectroscopy at 25°C. Absorbance values at 440 nm were normalized to the maximal increase *Δ*Abs in absorbance with the following equation, *Δ*Abs = $\mathrm{Abs_{obs}}$–$\mathrm{Abs_{ref}}$, where $\mathrm{Abs_{ref}}$ is absorbance of **5Zn** in the absence of **mP** under the same concentration of **5Zn** in the conditions of $\mathrm{Abs_{obs}}$. Job's plot was obtained by plotting *Δ*Abs values against mole fractions of **5Zn**.

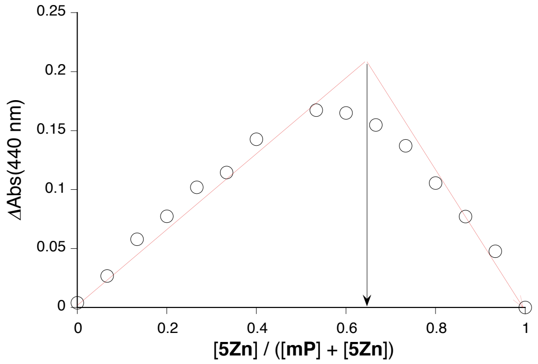

Figure S12. Job's plot for **5Zn–mP** complex formation.

An aliquot of a solution of **mP** was added to a solution of **5Zn** (1.5 x 10^{-6} M in CH_2Cl_2), and the resulting solutions were subjected to UV-vis. spectroscopy at 25°C. The spectrum was corrected with a dilution factor. The difference in absorbance of **5Zn** induced by the addition of **mP** was measured at 429 nm.

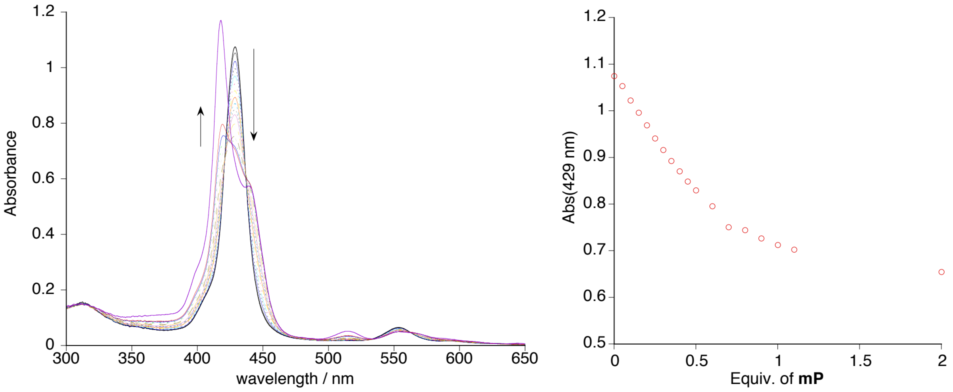

Figure S13. (left) Concentration dependence of the UV-vis absorption spectra in CH_2Cl_2 at 25°C: [**5Zn**] = 1.5 μM, [**mP**] = 0~3.0 μM. (right) A plot of the absorbance at 429 nm under various concentration of **mP**.

The free-energy change involved in an electron transfer process can be calculated by the Rehm–Weller equation (1):

$$\Delta_{ET}G^{0} = \left(E_{ox} - E_{red} - \frac{e^{2}}{4\pi\varepsilon_{0}\varepsilon_{r}r} \right) - \Delta E_{0,0} \quad (1)$$

$\Delta E_{0,0}$ is the excited-state energy, E_{ox} and E_{red} are the redox potentials of the donor and the acceptor. $e^2/4\pi\varepsilon_0\varepsilon_r r$ represents the Coulumbic energy associated with bringing separated radical ions at a distance r in a solvent of dielectric constant ε_r (r is the central distance of two porphyrin rings; here, we assume r = *ca*. 9 Å from the CPK model).

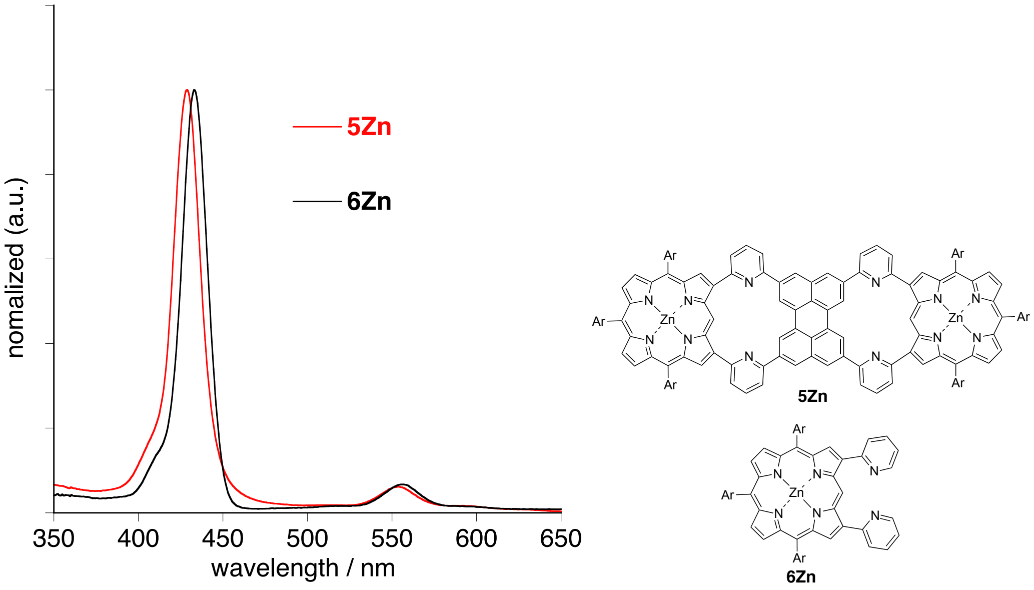

Figure S14. Comparison of absorption spectra of **5Zn** with **6Zn** in CH_2Cl_2.

Table S1. Crystal data and structure refinement for **5Ni**.

Empirical formula	$C_{164}H_{160}N_{12}Ni_2$	
Formula weight	2416.46	
Temperature	93(2) K	
Wavelength	1.54187 Å	
Crystal system	Triclinic	
Space group	*P* -1	
Unit cell dimensions	a = 20.6104(4) Å	α = 113.2820(8)°
	b = 28.4361(5) Å	β = 98.5654(9)°
	c = 32.8677(6) Å	γ = 95.3241(9)°
Volume	17251.5(6) $Å^3$	
Z	4	
Density (calculated)	0.930 Mg/m^3	
Absorption coefficient	0.613 mm^{-1}	
F(000)	5136	
Crystal size	0.30 x 0.10 x 0.05 mm^3	
Theta range for data collection	2.99 to 60.00°	
Index ranges	$-23 \le h \le 23$, $-31 \le k \le 31$, $-36 \le l \le 36$	
Reflections collected	165438	
Independent reflections	49820 [R(int) = 0.1035]	
Completeness to theta = 60.00°	97.3%	
Absorption correction	Semi-empirical from equivalents	
Max. and min. transmission	0.9700 and 0.8374	
Refinement method	Full-matrix least-squares on F^2	
Data / restraints / parameters	49820 / 2694 / 3190	
Goodness-of-fit on F^2	1.040	
Final R indices [$I > 2\sigma(I)$]	R_1 = 0.0971, $_wR_2$ = 0.1842	
R indices (all data)	R_1 = 0.2603, $_wR_2$ = 0.2069	
Largest diff. peak and hole	0.343 and –0.279 e.$Å^{-3}$	
CCDC number	865051	

*Explanation for a "level A" alert: Since the crystals contained many severely disordered solvent molecules with large unit cells, they gave only week diffractions, especially at the high θ range. However, these are not significant concern for the main skeletal structure. The contributions to the scattering arising from the presence of the disordered solvents in the crystal were removed by use of the utility SQUEEZE in the PLATON software package.

5. X-Ray Crystal Structure

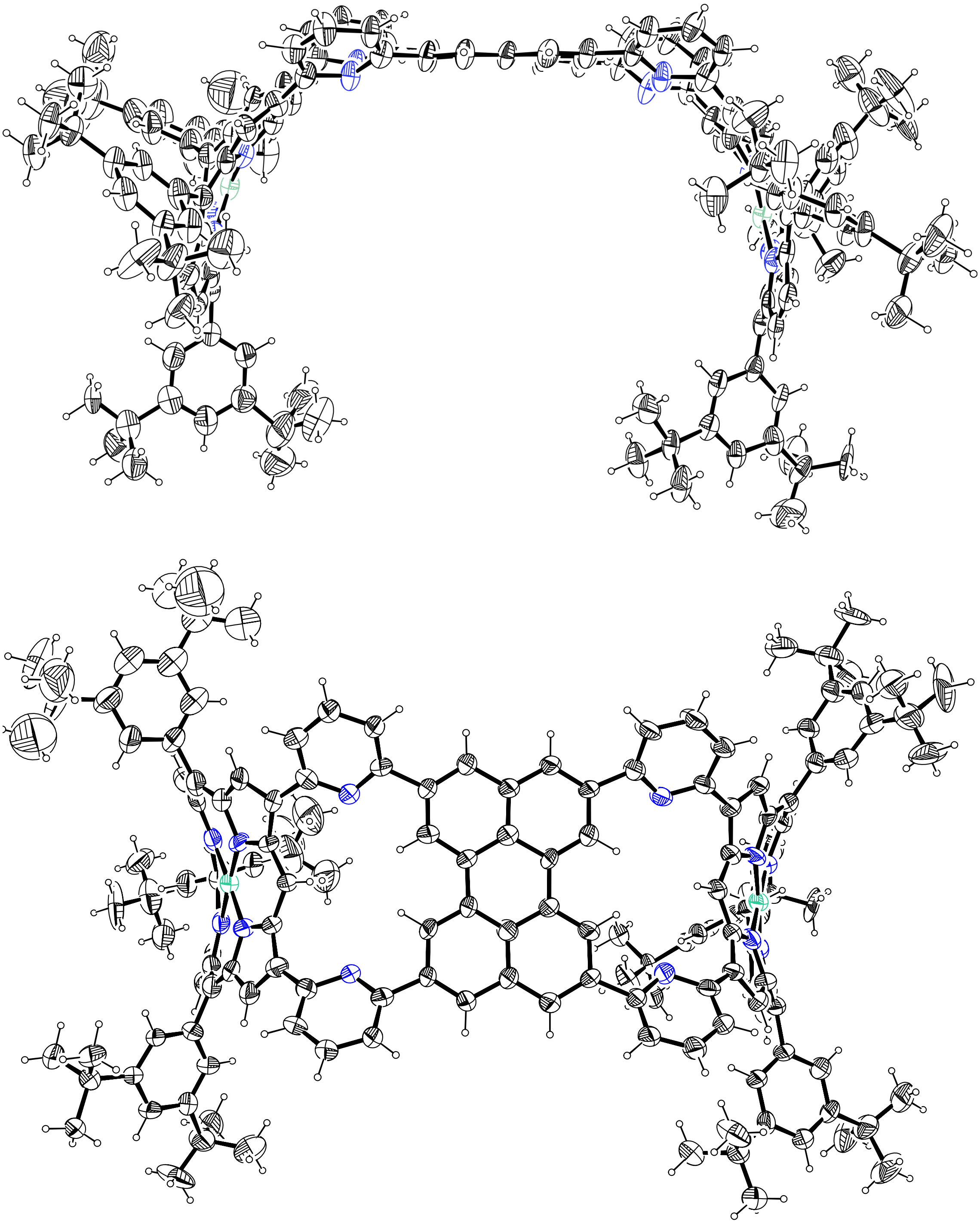

Figure S15. ORTEP drawing of the crystal structure of **5Ni** (triad A). Thermal ellipsoids were scaled to 20% probability.

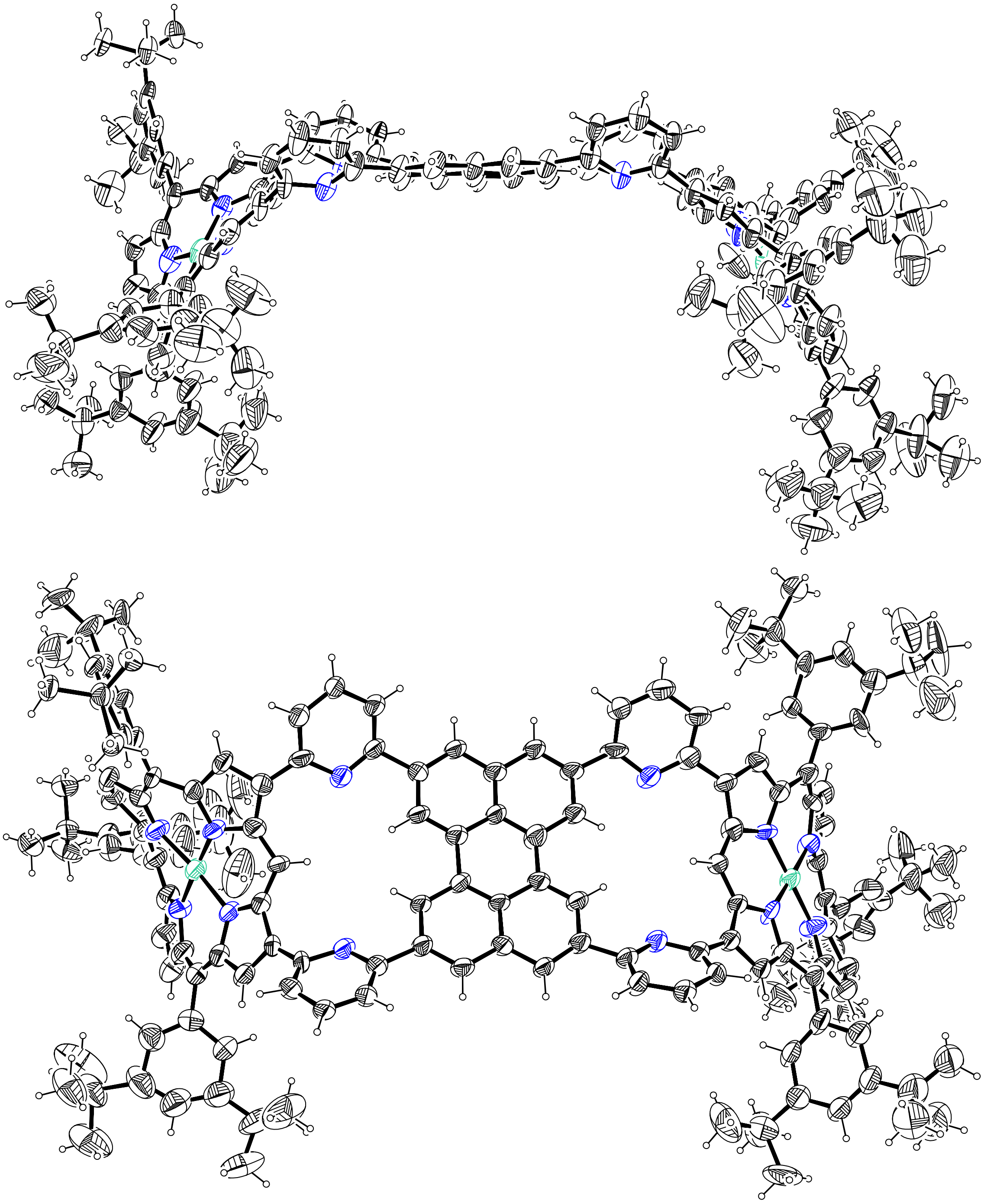

Figure S16. ORTEP drawing of the crystal structure of **5Ni** (triad B). Thermal ellipsoids were scaled to 20% probability.

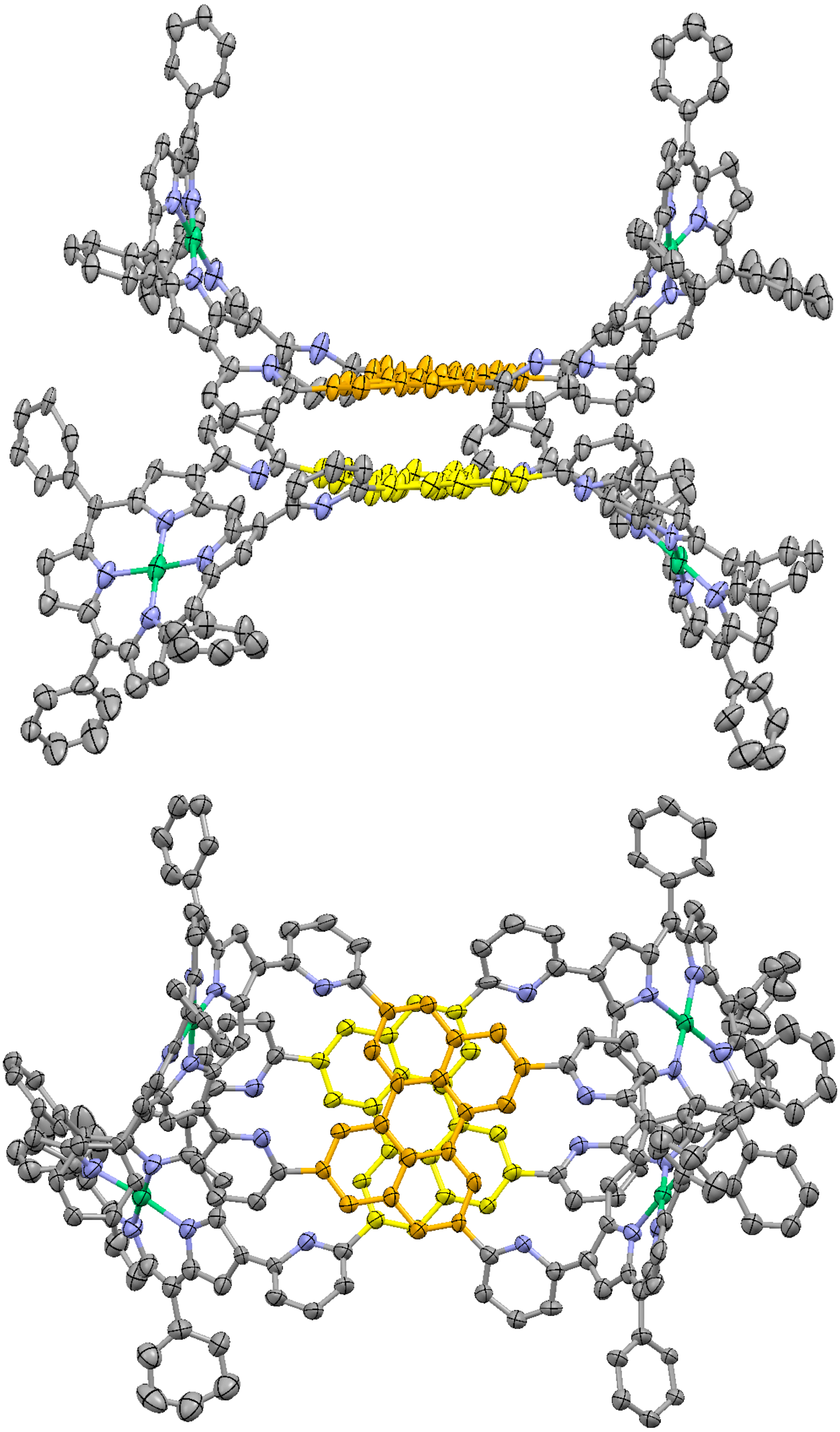

Figure S17. Dimeric form of **5Ni** in the solid state. Perylenes of trias A and B are coloured in orange and yellow, respectively. *tert*-Butyl groups and hydrogen atoms are omitted for clarity. The ellipsoids are scaled to the 20% probability.

6. References

[S1] SHELXL-97 and SHELXS-97, program for refinement of crystal structures from diffraction data, University of Gottingen, Gottingen (Germany); G. Sheldrick, T. Schneider, *Methods Enzymol.* 1997, **277**, 319.

[S2] D. N. Coventry, A. S. Batsanov, A. E. Goeta, J. A. K. Howard, T. B. Marder and R. N. Perutz, *Chem. Commun.*, 2005, 2172.

[S3] H. Hata, H. Shinokubo and A. Osuka, *J. Am. Chem. Soc.*, 2005, **127**, 8264.